HHS Public Access

Author manuscript

Anal Chim Acta. Author manuscript; available in PMC 2020 December 16.

Published in final edited form as:

Anal Chim Acta. 2019 December 16; 1089: 108–114. doi:10.1016/j.aca.2019.08.025.

Sorting by Interfacial Tension (SIFT): Label-Free Enzyme Sorting Using Droplet Microfluidics

Daniel G. Horvath[1], **Samuel Braza**[1], **Trevor Moore**[1], **Ching W. Pan**[1], **Lailai Zhu**[3,4], **On Shun Pak**[2], **Paul Abbyad**[1,*]

[1]Department of Chemistry and Biochemistry, Santa Clara University, Santa Clara, CA, 95053, USA

[2]Department of Mechanical Engineering, Santa Clara University, Santa Clara, CA, 95053, USA

[3]Department of Mechanical and Aerospace Engineering, Princeton University, Princeton, NJ 08544, USA

[4]KTH Mechanics, Stockholm, SE-10044, Sweden

Abstract

Droplet microfluidics has the ability to greatly increase the throughput of screening and sorting of enzymes by carrying reagents in picoliter droplets flowing in inert oils. It was found with the use of a specific surfactant, the interfacial tension of droplets can be very sensitive to droplet pH. This enables the sorting of droplets of different pH when confined droplets encounter a microfabricated trench. The device can be extended to sort enzymes, as a large number of enzymatic reactions lead to the production of an acidic or basic product and a concurrent change in solution pH. The progress of an enzymatic reaction is tracked from the position of a flowing train of droplets. We demonstrate the sorting of esterase isoenzymes based on their enzymatic activity. This label-free technology, that we dub droplet sorting by interfacial tension (SIFT), requires no active components and would have applications for enzyme sorting in high-throughput applications that include enzyme screening and directed evolution of enzymes.

Graphical Abstract

[*]corresponding author: Paul Abbyad, 500 El Camino Real, Santa Clara, CA 95053, (408) 554-6948, pabbyad@scu.edu.

Supporting Information Available: This material is available free of charge via the Internet at http://pubs.acs.org.

Declaration of interests

The authors declare that they have no known competing financial interests or personal relationships that could have appeared to influence the work reported in this paper.

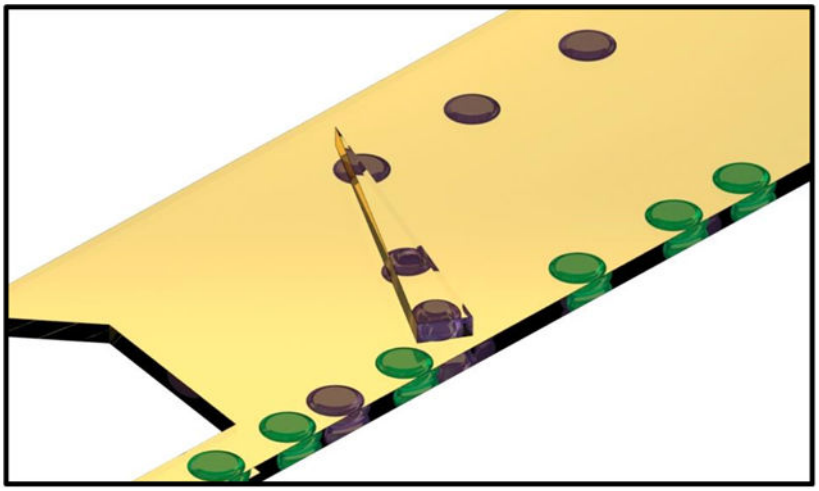

Introduction

Enzymes have the ability to accelerate diverse reactions in biochemistry but also find use for a wide range of applications in biotechnology, bioremediation, fuel production and synthesis of pharmaceuticals and fine chemicals. They frequently surpass conventional chemical catalysts utilizing milder reaction conditions while providing superior enantiomeric selectivity.[1] However, naturally occurring enzymes often lack the desired qualities and properties necessary for specific industrial or medical applications. While it is possible to engineer enzymes via rational design, this requires extensive prior knowledge of protein structures and function. Directed evolution of enzymes, in contrast, requires much less intimate knowledge of protein structure, and is a strong alternative for enzyme engineering.[2] In directed evolution, a library of mutated genes is created, and enzymes are screened via an assay for desired activity. Efficient screening methods are necessary to screen large libraries of combinatorial enzymes. Screening methods such as microtiter plate wells are limited to the screening of hundreds or thousands of enzymes. However, many screening applications require the sorting of libraries of tens of millions of variants.

To meet this challenge, high-throughput techniques have been developed to sort enzymes using fluorescence activated cell sorting (FACS) or fluorescently activated droplet sorting (FADS)[3]. FACS sorts cells containing distinct enzymes that are either contained in the cell or tethered to the cell surface. However, a limitation is that the assay output must remain in the cell or be linked to the cell.[4] In contrast, FADS encapsulates both the enzyme and the corresponding cell (or DNA for cell free systems) within a picoliter droplet in oil. To select enzymes, droplet sorters primarily use electric fields to select droplets over a defined signal threshold, [5,6] with recently reported sorting rates of 30 kHz.[7] Although powerful, both of these techniques are expensive; they require the observation of the cell or droplet (usually by fluorescence) and synchronization with an active component for selection or sorting.[4,8] FADS also requires a change in fluorescence upon enzymatic conversion.[8] Very few natural enzyme substrates are suitably equipped with a fluorescent moiety and development of a

fluorescent readout system is both tedious and costly. There is also a real risk of artifacts based on selection on proprieties of the probe rather than the desired target.

Hundreds of enzymes lead to the production of an acidic or basic product and include the family of enzymes such as esterases, lipases and dehalogenases.[9,10] The worldwide demand for these enzymes can be measured in billions of dollars.[9,11] The evolution or screening of these enzymes has great commercial interest for applications including organic synthesis for food and pharmaceuticals,[9,12] and the bioremediation of pollutants and warfare agents.[9,13] The activity of these enzymes are routinely measured by a change in solution pH, often observed with a colorimetric pH indicator, due to product formation.[12,14-16] This change in solution pH can also be used for selecting and sorting enzymes based on their activity. Droplet microfluidics allows for high throughput screening on a chip as each enzyme variant can be contained within a nanoliter droplet.

We present here a label-free device that uses the change of droplet pH from enzymatic product formation for enzyme selection. The sorting mechanism utilizes a change in droplet interfacial tension resulting from pH change to control droplet flow position. This passive strategy eliminates the need for a probe or costly active droplet sorting technology. We dubbed this droplet sorting strategy: *Sorting by Interfacial Tension* (SIFT). This technique was recently used for single-cell encapsulation and live cell sorting based on metabolism.[17] We show here how the technique can be applied to enzyme sorting. The progress of an enzymatic reaction is determined from the position of a flowing train of droplets. We demonstrate selection of enzymes based on enzymatic activity, an application relevant for use in high-throughput applications that include enzyme screening and directed evolution of enzymes.

Materials and Methods

Pendant Drop:

Interfacial tension measurements were performed on FTA 1000 (First Ten Angstroms) goniometer. Aqueous droplets in oil were produced using a 20 gauge j-needle. Droplets were allowed to equilibrate for approximately 7 minutes prior to measurement. QX100 Droplet Generation Oil (Biorad) was diluted 100X with perfluorinated oil, NOVEC 7500 (3M), as aqueous droplets in less diluted QX100 Droplet Generation Oil had very low interfacial tension that detached within seconds from the needle. Interfacial tension was determined by fits to the droplet shape using First Ten Angstroms analysis software.

Microfluidic Device:

Polydimethylsiloxane (PDMS) microfluidic chips with channel depth modulations were fabricated using the dry-film photoresist soft lithography technique described by Stephan *et al.*[18]. This technique enabled rapid prototyping of multi-level structures. The PDMS chips were then plasma-bonded to a glass slide. To render the internal channel surface hydrophobic, Novec™ 1720 Electronic Grade Coating (3M) was flowed into the microchannel and the chip was heated for 30 minutes at 150°C. The surface treatment prevented wetting and contact of the aqueous droplets with the channel walls.

Measurements:

Porcine liver esterases and phenyl acetate were obtained from Sigma Aldrich. Enzyme solutions were prepared in phosphate buffer (137 mM NaCl, 10 mM phosphate). To achieve the initial pH of phosphate buffer without varying the ionic strength, solutions of 10mM sodium phosphate dibasic and sodium phosphate monobasic were mixed to the desired pH. Aqueous droplets in oil formed from a flow focuser were flowed into a 3 mm wide channel containing the sorting rail. The oil used in all experiments was QX100 Droplet Generation Oil (Biorad) diluted 2.5X with Novec 7500 (3M). This dilution factor was used as it led to the most efficient sorting while minimizing droplet coalescence and wetting. Fluid flow was controlled using computer-controlled syringe pumps (Nemesys, Cetoni). Images were taken with a 4X objective on an inverted fluorescence microscope (Olympus IX-50) equipped with shuttered LED fluorescence excitation source (Sola SE-II). Concurrently as on-chip experiments, the pH of enzyme solutions was monitored off-chip using a semi-micro pH electrode (Orion 9110DJWP Thermo Fischer). Care was taken to ensure that pH readings and video images were properly synchronized in time.

Simulations:

To estimate the magnitude of the entrainment flow in the chip, a threedimensional model was created with the same geometry of the chip without channel height modulations. The presence of the trench was assumed to have negligible influence on the overall magnitude of the entrainment flow. The flow was simulated using commercial finite-element software COMSOL Multiphysics by solving the Stokes equation. For boundary conditions, the same flow rates used in the experiments were prescribed at the two inlets, with pressure set to zero at the outlet and no-slip condition on all channel walls.

Results and Discussion

In droplet microfluidics,[19] biological and chemical reagents are encapsulated in aqueous droplets transported in inert oil. The ability to analyze large numbers of discrete nanoliter to picoliter droplets has increased throughput in a broad range of biological applications that include directed evolution,[6,20] digital PCR,[21] drug screening[22] and large-scale biological assays.[6,22-24] Perfluorinated oils are commonly used as the external oil for many droplet applications as they limit the transfer of droplet content to the oil phase while displaying good biocompatibility and oxygen transport for applications in cellular culture. Typically, the surfactants used with perfluorinated oil are polymers consisting of both a hydrophilic and perfluorinated moieties.[25] Surfactants play a crucial role in droplet microfluidics. They reduce droplet interfacial tension (surface tension between the aqueous droplet and oil) and thus aid in the formation of droplets and inhibit droplet coalescence and wetting of droplets on channel walls. In a few cases, surfactants have additional functions, having been used in droplet microfluidics as fluorescent probes of the droplet interface or as catalysts for chemical reactions.[26,27] The physical properties of aqueous droplets in oil have been used for analyte detection or sorting. For example, the lab of Amar Basu used changes in surface tension to sort droplets with and without bovine serum albumin based on migration in a surfactant gradient.[28,29]

It was observed that for aqueous droplets in the external oil, QX100 Droplet Generation Oil (Biorad) a product designed for use with the QX200/QX100 droplet digital PCR system, the physical properties of droplets are very sensitive to pH. In particular, a decrease in pH can lead to a large increase in interfacial tension as measured by pendant droplet (Fig. 1a). These pendant drop measurements show the trend rather than the values of interfacial tension on chip. To produce consistent results through the entire pH range, 100 fold diluted surfactant solutions were measured. Furthermore, pendant droplet measurements on similar systems can take hours to stabilize.[30]

The change in interfacial tension with pH occurs in a range (6-10) that is particularly relevant for biological samples. This dependence was observed in all aqueous solutions studied including buffer (PBS) and rich media (DMEM). This sensitivity to pH was not observed for neat solvent nor for other common surfactants used in combination with perfluorinated oils such as 008 fluorosurfactant (Ran Technologies) or Picosurf I and II (Dolomite Microfluidics). A probable cause of the pH sensitivity is a change in fluorosurfactant protonation state with pH. Many fluorosurfactants with acidic or basic moieties in the headgroup have been developed to stabilize emulsions.[25,31] These include head groups containing phosphates, carboxylic acids and amines (primary, secondary and tertiary). Phosphates and amines would have a pKa that would lead to a mix of neutral and charged surfactant near neutral pH. A change in protonation state and charge can drastically change the surface properties of the surfactant including the critical micelle concentration (CMC), transport properties, and surface tension.[32,33] For example, amine containing head groups show marked increase in surface tension as the pH was decreased in aqueous solutions.[32,33] At the same surfactant concentration, at low pH the surfactant would exist as a dispersed monomer while at high pH the surfactant assembles at the water/oil interface.[33] The proprietary surfactant structure of QX100 Droplet Generation Oil however hinders confirmation of the exact source for the observed pH sensitivity. The change of interfacial tension of the droplet with pH provides a handle for droplet sorting or isolation.

A schematic of the droplet sorter is presented in Figure 1b and leverage changes in surface tension to sort droplets using the general techniques of “Rails and Anchors”.[34-36] Dimensions and geometry of the droplet sorting region is provided in supplemental Figure S1. Without additional forces, droplets take the shape that minimizes their surface area, a sphere. In this device, the channel height (50 μm) is smaller than the droplet diameter (80-150 μm), the droplets are therefore pancake shaped, squeezed by the top and bottom surfaces of the channel. Droplets, produced with flow focusers,[19] are introduced in the lower portion of a wide channel and enter the microfabricated trench, the rail, which has a greater channel height (65 μm). The droplets change shape when in the rail, reducing their overall surface area. The retaining force, keeping the drop in the rail, is proportional to this change in surface area. Using a simple model provided in the supplemental information,[36,37] it is estimated that under our experimental conditions it requires interfacial tension in the order of one dyne/cm to hold a droplet on the rail. The flow of oil exerts a drag force from the left to right on the droplet and also pushes the droplet up along the rail that is oriented at 45° with respect to the flow direction.

While part of the oil flow is provided from the droplet inlet (5-10μL/min), the majority of the flow comes from an extra oil inlet, the Oil Entrainment Inlet (top left of schematic Fig. 1b) that is adjusted between 25 and 60 μL/min. The Oil Entrainment Inlet allows an independent control of the total entrainment flow in the sorting region of the device and hence the hydrodynamic drag.

When the force of drag overcomes the retaining force, which is proportional to the interfacial tension, the droplet is pushed off the rail. An increasing oil entrainment flow along the length of the rail is generated as there is substantially higher flow rate (e.g., 30 μL/min) at the Oil Entrainment Inlet than the other inlet (e.g., 6 μL/min). Under these inlet flow rates, flow simulations by COMSOL Multiphysics suggest that the entrainment flow speed can increase from approximately 3 mm/s at the entrance to 7 mm/s at the end of the rail (supplemental Figure S2). The droplets thus experience increasing fluid drag along the length of the rail due to the increasing oil entrainment flow. As a result, droplets of different interfacial tension will get pushed off the rail at different positions. Furthermore, the rail is tapered. As the droplet follows the rail upwards, the rail width eventually becomes narrower than the droplet diameter and droplets are only partially in the rail (top two purple droplets on rail in Fig. 1b). The shape change results in an increasing surface area as droplets follow the rail. The decreasing retaining force also leads to different exit positions of droplets based on interfacial tension. Droplets of very high interfacial tension leave the rail at the top when it reaches a point. In this way, droplets of lower surface tension (green droplets) are pushed off the rail at the bottom while droplets of higher interfacial tension (purple droplets) exit at a higher position. This principal allows for efficient sorting of droplets based on interfacial tension and thus pH.

The sorting of droplets of different pH is shown in Figure 2 and supplemental video S1. All droplets enter at the bottom portion of the sorting region. Droplets at lower pH have higher interfacial tension. These droplets follow the rail for most of its length and are displaced laterally in the channel (white droplets). Droplets at higher pH and lower interfacial tension are only slightly displaced laterally (clear droplets). The flow rate of the Oil Entrainment Inlet was adjusted manually to maximize the difference in laterally displacement between the two droplet populations. For the pH range studied, it was generally set to a flow rate between 25 and 60 μL/min.

Since the sorting is based on a physical property of the droplet it is reproducible, predictable and robust. However, sorting errors can occur, primarily due to droplet interactions. In the case of a binary population, as in Figure 2, droplet bunching can occasionally push off a droplet earlier than expected for a given droplet pH (false negative). For the representative data presented in Figure 2 and supplemental video S1, this occurred at a rate of 3.4 % for the low pH droplets (8 droplets of a total of 232). Likewise a droplet at high pH can potentially be carried up the rail if positioned behind several droplet of low pH (false positive). However, this type of error was easily avoided and no false positives were observed for the high pH droplets (210 droplets). Both these errors are minimized or eliminated by optimizing oils flows to ensure proper spacing between the individual droplets to be sorted. Under optimized flow parameters, droplets can be sorted indefinitely with errors similar to reported above.

We were successful in sorting droplets in the pH range of around 6.0 to 7.5 with a difference of pH of 0.4. The surfactant pluronic F68 can be added to the aqueous phase to lower the overall interfacial tension. This is useful near the lower end of the pH range, around 6.0-6.4, when the high interfacial tension would otherwise cause all droplets to follow the rail upwards. Our experiments have shown that droplets separated by as little as 0.2 pH units will leave the rail at different lateral positions. The current device can sort droplets at a maximum rate of about 30 Hz.

The technique can be used as a label-free method of measuring reaction progress for chemical or enzymatic reactions by tracking droplet position. This is demonstrated by the enzymatic hydrolysis of phenyl acetate by esterase (porcine liver) to produce acetic acid (Figure 3 and supplementary video S2). The production of the product, acetic acid, leads to an acidification of the buffered solution over time. The pH of the enzymatic solution was concurrently monitored off-chip with a pH meter.

As the reaction proceeds, droplets are further diverted by the rail and flow at a higher position in the channel (Fig. 3a). The droplet size remains constant throughout the experiment. Occasional bursts of droplets on the rail lead to droplets pushed off rail before anticipated. The change in lateral position, from the bottom to the top of the rail, occurs in a relatively narrow pH range as the pH drops from pH 7.0 to 6.8.

The experiment was run at two different enzyme concentrations under conditions of high substrate concentration, high above the enzyme K_m that is in the micromolar range[38] thus ensuring enzyme saturation. Under these conditions, the pH change over time is largely linear and proportional to the enzyme concentration (Fig 3b). While the lateral displacement in the channel occurs at different times (Fig. 3c) for different enzyme concentrations in the sorting device, it occurs within a very similar pH range (Fig. 3d). This indicates that pH is the dominant factor in droplet lateral displacement. The buffer capacity used, in this case 10mM phosphate, can be tuned to modulate sensitivity of the device to pH changes due to product formation. Using lower buffer concentrations will lead to a faster pH change for the same enzyme conditions.

SIFT can be used to sort enzymes based on their enzymatic activity. Droplets containing more efficient enzymes produce greater quantities of acidic product and thus undergo greater lateral movement in relation to flow direction to enzymes with lower enzyme activity. This is demonstrated by the cleavage of phenyl acetate by two different isoenzymes, Esterase Isoenzyme 4 and Esterase Isoenzyme 5. The reaction was initiated at the same time and initial pH for both isoenzymes. Esterase Isoenzyme 5 has greater enzyme activity than Esterase Isoenzyme 4 leading to a larger drop of pH. At 35 minutes of reaction time, droplets were produced containing each enzyme. At this time, the production of product led to a difference in pH. Droplets containing Esterase Isoenzyme 5 were at pH 6.2 and Esterase Isoenzyme 4 were at pH 6.6. In the sorting device, droplets containing Esterase Isoenzyme 4 (white droplets) were only slightly diverted by the rail while droplets containing Esterase Isoenzyme 5 (clear droplets) were diverted laterally by the rail (Fig. 4 and supplementary video S3). Optimizing flow rates allowed an efficient sorting. No errors were observed on the sorting of 673 droplets containing Esterase 4 and 596 droplets containing Esterase 5. In

the entry passage, a small fraction of Esterase 4 droplets (3.7%) split into two droplets however these smaller droplets were corrected sorted.

The device was also shown to be effective for other enzymes including the sorting based on halogen cleavage activity by haloalkane dehalogenase variants, an application relevant for bioremediation (data not shown).[13] Multiple chip outlets can be used to collect droplets containing different enzyme variants. Using this strategy, closely related enzymes can be sorted and collected based on their activity to a designated substrate, thus enabling the use of the technique for enzyme screening or directed evolution.

Conclusions

We have shown that pH can directly influence the interfacial tension of aqueous droplets in perfluorinated oils. Based on this relationship, we have developed a robust, label-free method of sorting droplets by their pH called SIFT. The power of the passive sorting strategy is that it selects based on physical changes in droplet properties. As a result, sorting is very predictable, and is relatively error-free. The sensitivity of the device is easily modulated by changing the buffer capacity of solution. The technique forgoes the excitation laser, detector, active sorter and related electronics, and fluorescent label that are intrinsic to other microfluidic droplet sorters. This makes SIFT an inexpensive solution with the sorting capacity incorporated in the chip channel geometry.

As the first iteration of this sorter, there is still room for optimization of both throughput and sensitivity. The current device sorts droplets at a rate of about 30 Hz or about 100,000 droplets per hour. Many applications in enzyme screening would require higher throughput. The first design was not designed for maximum throughput. There are likely improvements that can be achieved by optimizing flow channel geometries and flow properties using numerical simulations. Furthermore, the lack of active sorting components enables sorting elements to be easily added with little extra cost. This enables sorting elements to be reproduced and used in parallel to achieve high throughput.

The method is relevant for enzymes that produce acidic (or basic) products that include the family of enzymes such as esterases, lipases and dehalogenases. As a label-free technique, SIFT can be used directly with the desired target without modification. Moreover, it can be used with many substrates for each enzyme, including many that could not be easily labeled. The technique removes the expense and time in developing a fluorescence enzyme readout system. It also avoids potential artifacts linked to selection on proprieties of the probe rather than the intended substrate.

The technique has potential as a robust droplet sorting element for high-throughput selection or direction evolution of enzymes, especially for systems where screening numbers exceed the reasonable capacity of microtiter plate wells (greater than 10^4 enzyme variants). Droplets have been used to sort large libraries of enzymes[6,20] and is attractive as it confines and thus links the phenotype and genotype within the droplet for both cell and cell-free enzyme expression systems. Droplets containing substrate and enzyme could be combined on chip via droplet fusion using existing techniques.[22] Incubation of droplets prior to sorting would

allow for a pH difference to emerge in droplets containing enzymes with high activity. After a defined incubation time, droplets would be distributed among the droplet sorters used in parallel (or in series for more discriminatory sorting) for greater throughput. SIFT would present a simple enzyme sorting strategy that removes the need of labels or specialized equipment for the selection and directed evolution of a large family of enzymes that result in acidic or basic products.

Supplementary Material

Refer to Web version on PubMed Central for supplementary material.

Acknowledgements

We acknowledge helpful discussions with Christopher Weber of the Department of Physics at Santa Clara University. SB acknowledges generous funding from ALZA through the ALZA Corporation Science Scholar program. We would also like to thank International Electronic Components Inc. for their generous donation of dry photoresist. Paul Abbyad is supported for this project by a National Science Foundation Career Award, Grant Number 1751861 and the National Institutes of Health under grant 1R15GM129674-01.

References

1. Kuchner O & Arnold FH Directed evolution of enzyme catalysts. Trends Biotechnol. 15, 523–530 (1997). [PubMed: 9418307]
2. Arnold FH Design by Directed Evolution. Acc. Chem. Res. 31, 125–131 (1998).
3. Baret J-C, Miller OJ, Taly V, Ryckelynck M, El-Harrak A, Frenz L, Rick C, Samuels ML, Hutchison JB, Agresti JJ, Link DR, Weitz DA & Griffiths AD Fluorescence-activated droplet sorting (FADS): efficient microfluidic cell sorting based on enzymatic activity. Lab Chip 9, 1850–8 (2009). [PubMed: 19532959]
4. Longwell CK, Labanieh L & Cochran JR High-throughput screening technologies for enzyme engineering. Curr. Opin. Biotechnol. 48, 196–202 (2017). [PubMed: 28624724]
5. Colin PY, Zinchenko A & Hollfelder F Enzyme engineering in biomimetic compartments. Curr. Opin. Struct. Biol. 33, 42–51 (2015). [PubMed: 26311177]
6. Agresti JJ, Antipov E, Abate AR, Ahn K, Rowat AC, Baret J-C, Marquez M, Klibanov AM, Griffiths AD & Weitz DA Ultrahigh- throughput screening in drop-based microfluidics for directed evolution. Proc. Natl. Acad. Sci. 107, 4004–9 (2010). [PubMed: 20142500]
7. Sciambi A & Abate AR Accurate microfluidic sorting of droplets at 30 kHz. Lab Chip 15, 47–51 (2015). [PubMed: 25352174]
8. Packer MS & Liu DR Methods for the directed evolution of proteins. Nat. Rev. Genet. 16, 379–394 (2015). [PubMed: 26055155]
9. Peña-García C, Martínez-Martínez M, Reyes-Duarte D & Ferrer M High Throughput Screening of Esterases, Lipases and Phospholipases in Mutant and Metagenomic Libraries: A Review. Comb. Chem. High Throughput Screen. 19, 605–615 (2016). [PubMed: 26552433]
10. McDonald AG, Boyce S, Moss GP, Dixon HBF & Tipton KF ExplorEnz: A MySQL database of the IUBMB enzyme nomenclature. BMC Biochem. 8, 1–7 (2007). [PubMed: 17224065]
11. Li S, Yang X, Yang S, Zhu M & Wang X Technology prospecting on enzymes: application, marketing and engineering. Comput. Struct. Biotechnol. J. 2, e201209017 (2012). [PubMed: 24688658]
12. May O, Nguyen PT & Arnold FH Inverting enantioselectivity by directed evolution of hydantoinase for improved production of L-methionine. Nat. Biotechnol. 18, 317–320 (2000). [PubMed: 10700149]
13. Koudelakova T, Bidmanova S, Dvorak P, Pavelka A, Chaloupkova R, Prokop Z & Damborsky J Haloalkane dehalogenases: Biotechnological applications. Biotechnology Journal 8, 32–45 (2013). [PubMed: 22965918]

14. Morís-Varas F, Shah A, Aikens J, Nadkarni NP, Rozzell JD & Demirjian DC Visualization of enzyme-catalyzed reactions using pH indicators: Rapid screening of hydrolase libraries and estimation of the enantioselectivity. Bioorganic Med. Chem. 7, 2183–2188 (1999)
15. Holloway P, Trevors JT & Lee H A colorimetric assay for detecting haloalkane dehalogenase activity. J. Microbiol. Methods 32, 31–36 (1998).
16. Phillips TM, Seech AG, Lee H & Trevors JT Colorimetric assay for Lindane dechlorination by bacteria. J. Microbiol. Methods 47, 181–188 (2001). [PubMed: 11576682]
17. Pan CW, Horvath DG, Braza S, Moore T, Lynch A, Feit C & Abbyad P Sorting by interfacial tension (SIFT): label-free selection of live cells based on single-cell metabolism. Lab Chip 19, 1344–1351 (2019). [PubMed: 30849144]
18. Stephan K, Pittet P, Renaud L, Kleimann P, Morin P, Ouaini N & Ferrigno R Fast prototyping using a dry film photoresist: microfabrication of soft- lithography masters for microfluidic structures. J. Micromech. Microeng. 17, N69 (2007).
19. Thorsen T, Roberts RW, Arnold FH & Quake SR Dynamic Pattern Formation in a Vesicle-Generating Microfluidic Device. Phys. Rev. Lett. 86, 4163–4166 (2001). [PubMed: 11328121]
20. Obexer R, Godina A, Garrabou X, Mittl PRE, Baker D, Griffiths AD & Hilvert D Emergence of a catalytic tetrad during evolution of a highly active artificial aldolase. Nat. Chem. 9, 50–56 (2017). [PubMed: 27995916]
21. Pekin D, Skhiri Y, Baret J-C, Le Corre D, Mazutis L, Salem C.Ben, Millot F, El Harrak A, Hutchison JB, Larson JW, Link DR, Laurent-Puig P, Griffiths AD & Taly V Quantitative and sensitive detection of rare mutations using droplet-based microfluidics. Lab Chip 11, 2156–66 (2011). [PubMed: 21594292]
22. Brouzes E, Medkova M, Savenelli N, Marran D, Twardowski M, Hutchison JB, Rothberg JM, Link DR, Perrimon N & Samuels ML Droplet microfluidic technology for single-cell high-throughput screening. Proc. Natl. Acad. Sci. 106, 14195–14200 (2009). [PubMed: 19617544]
23. Debs B.El, Utharala R, Balyasnikova IV, Griffiths AD & Merten CA Functional single-cell hybridoma screening using droplet-based microfluidics. Proc. Natl. Acad. Sci. 109, 11570–11575 (2012). [PubMed: 22753519]
24. Huebner A, Bratton D, Whyte G, Yang M, Demello AJ, Abell C & Hollfelder F Static microdroplet arrays: a microfluidic device for droplet trapping, incubation and release for enzymatic and cell-based assays. Lab Chip 9, 692–698 (2009). [PubMed: 19224019]
25. Clausell-Tormos J, Lieber D, Baret JC, El-Harrak A, Miller OJ, Frenz L, Blouwolff J, Humphry KJ, Koster S, Duan H, Holze C, Weitz DA, Griffiths AD & Merten CA Droplet-Based Microfluidic Platforms for the Encapsulation and Screening of Mammalian Cells and Multicellular Organisms. Chem. Biol. 15, 427–437 (2008). [PubMed: 18482695]
26. Theberge AB, Whyte G, Frenzel M, Fidalgo LM, Wootton RCR & Huck WTS Suzuki–Miyaura coupling reactions in aqueous microdroplets with catalytically active fluorous interfaces. Chem. Commun. 6225–6227 (2009).
27. Baret JC, Kleinschmidt F, El Harrak A & Griffiths AD Kinetic Aspects of Emulsion Stabilization by Surfactants: A Microfluidic Analysis. Langmuir 25, 28 6088–6093 (2009). [PubMed: 19292501]
28. Kurup GK & Basu AS Passive, Label-Free Droplet Sorting by Chemical Composition Using Tensiophoresis. Micro Total Anal. Syst. 2012 76–78 (2012).
29. Kurup GK & Basu AS Deterministic Protein Extraction from Droplets using Interfacial Drag and Tensiophoresis. Micro Total Anal. Syst. 2013 1344–1346 (2013).
30. Brosseau Q, Vrignon J & Baret J-C Microfluidic Dynamic Interfacial Tensiometry (μDIT). Soft Matter 10, 3066–76 (2014). [PubMed: 24695668]
31. Holtze C, Guerra RE, Agresti J, Weitz DA, Ahn K, Hutchison JB, Griffiths AD, El-Harrak A, Miller OJ, Baret J-C, Taly V, Rychellynck M & Merten C Fluorocarbon Emulsion Stabilizing Surfactants. EP 2 077 912(2007).
32. Wang W, Lu W & Jiang L Influence of pH on the aggregation morphology of a novel surfactant with single hydrocarbon chain and multi-amine headgroups. J. Phys. Chem. B 112, 1409–1413 (2008). [PubMed: 18197654]

33. Jiang Z, Li X, Yang G, Cheng L, Cai B, Yang Y & Dong J PH-responsive surface activity and solubilization with novel pyrrolidone-based gemini surfactants. Langmuir 28, 7174–7181 (2012). [PubMed: 22502732]

34. Abbyad P, Dangla R, Alexandrou A & Baroud CN Rails and anchors: guiding and trapping droplet microreactors in two dimensions. Lab Chip 11, 813–821 (2011). [PubMed: 21060946]

35. Fradet E, McDougall C, Abbyad P, Dangla R, McGloin D & Baroud CN Combining rails and anchors with laser forcing for selective manipulation within 2D droplet arrays. Lab Chip 11, 4228–34 (2011). [PubMed: 22045291]

36. Rashid Z, Erten A, Morova B, Muradoglu M, Jonáš A & Kiraz A Passive sorting of emulsion droplets with different interfacial properties using laser - patterned surfaces. Microfluid. Nanofluidics 23, (2019).

37. Dangla R, Lee S & Baroud CN Trapping Microfluidic Drops in Wells of Surface Energy. Phys. Rev. Lett. 107, 124501 (2011). [PubMed: 22026771]

38. Junge W & Heymann E Characterization of the Isoenzymes of Pig Liver Esterase 2. Kinetic Studies. Eur. J. Biochem. 95, 519–525 (1979). [PubMed: 446478]

Highlights

- A novel droplet microfluidic device allows the sorting of droplets based on pH without the use of labels or active components
- The technique is used to view the progression of an enzyme reaction via the flow position of droplets
- The device is used to sort droplets containing esterase isoenzymes based on their enzymatic activity

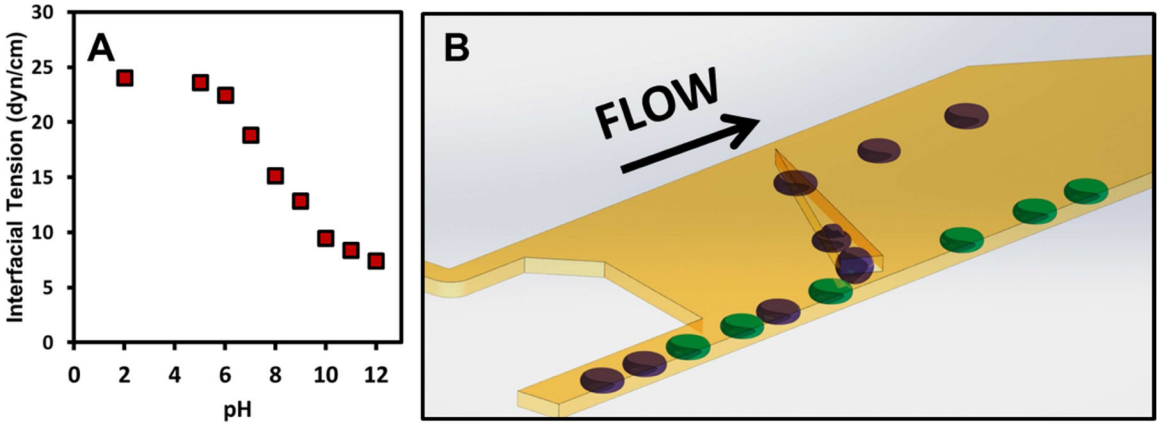

Figure 1.

a) Interfacial tension as of function of pH for droplets of phosphate buffered saline in QX100 Droplet Generation Oil diluted 100 fold by volume with Novec 7500. **b)** Schematic of droplet sorter using a tapered rail oriented at 45° in relation to the direction of flow. Low pH droplets are indicated in purple while high pH droplets indicated in green. Droplets enter from bottom left channel. Droplets of high pH (low interfacial tension) are only slightly deflected by the rail. However, droplets of low pH (high interfacial tension) enter the rail and follow the rail upwards. The top left inlet, the Oil Entrainment Inlet, allows an independent control of the hydrodynamic drag in the sorting region of the device. The change in shape of the droplets in the rail is exaggerated for illustrative purposes.

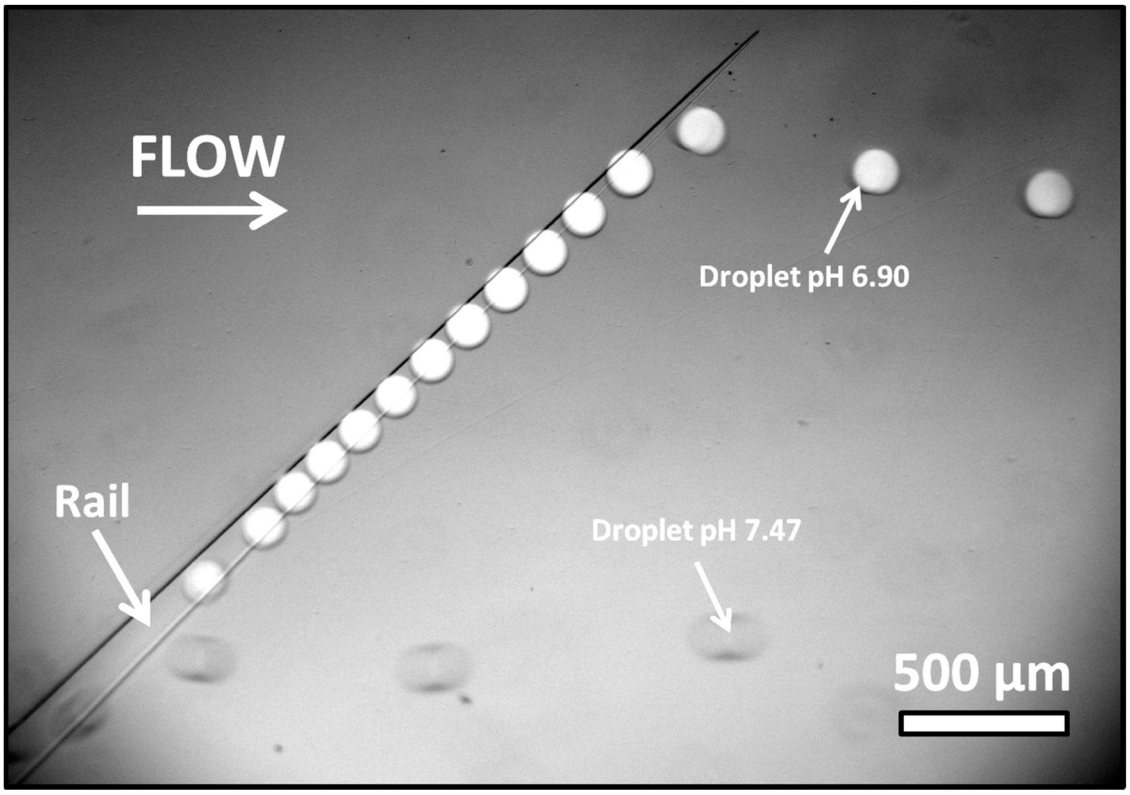

Figure 2.

Selection of droplets of different pH using SIFT. Droplets enter from bottom left of image. White droplets at lower pH (pH = 6.90) of higher interfacial tension follow the rail upwards. Clear droplets at higher pH (pH = 7.47) are only slightly deflected by the rail. A small amount of fluorescein is added to the droplets at pH = 6.90 to identify the two droplet populations.

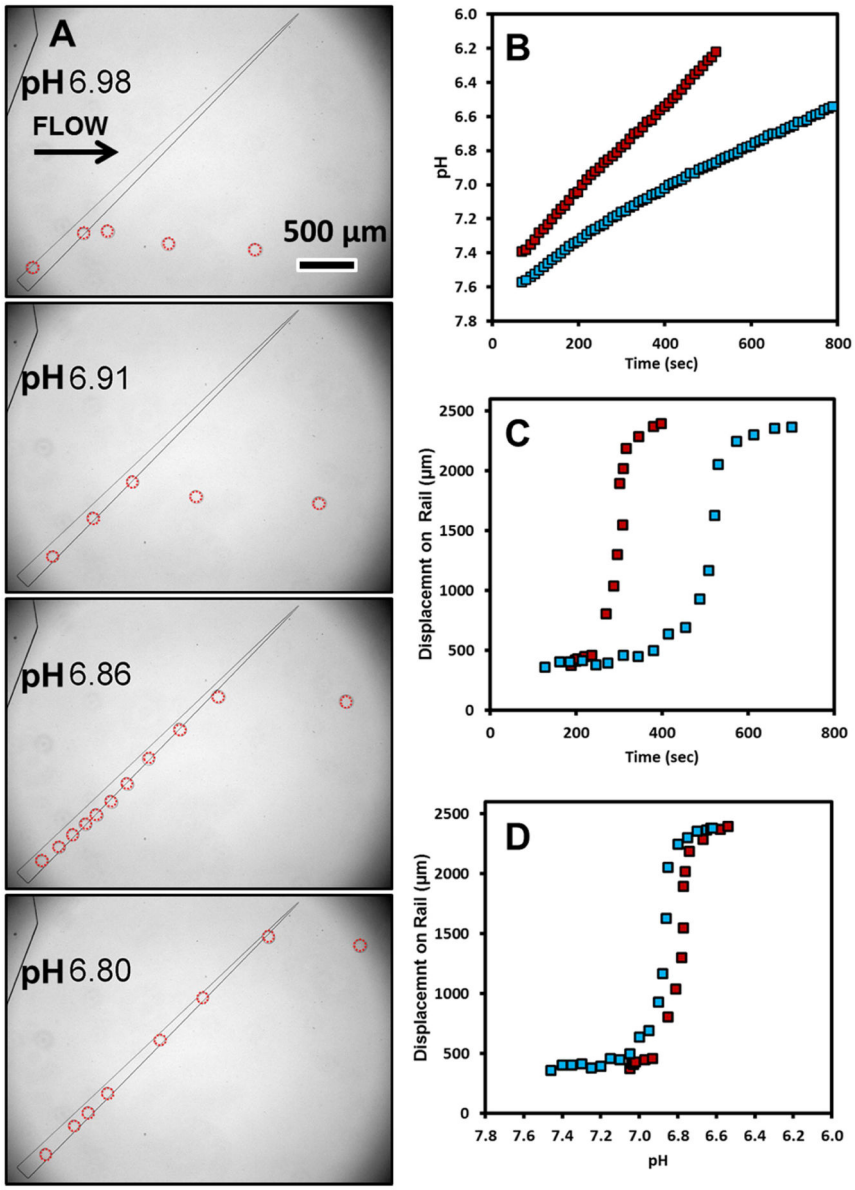

Figure 3.

a) Image Sequence of the movement of droplet from the enzymatic hydrolysis of phenyl acetate (0.102M) by porcine liver esterase (0.36µM) to produce acetic acid. Droplets are outlined in red in images for clarity. Enzymatic formation of the product leads to an acidification of the droplet and a larger lateral displacement relative to the flow direction. **b)** Change in pH over time from breakdown of phenyl acetate by porcine liver esterase at 0.89µM solution (red) and at 0.36µM (blue). **c)** Displacement of droplets along rail as function of time and **d)** pH

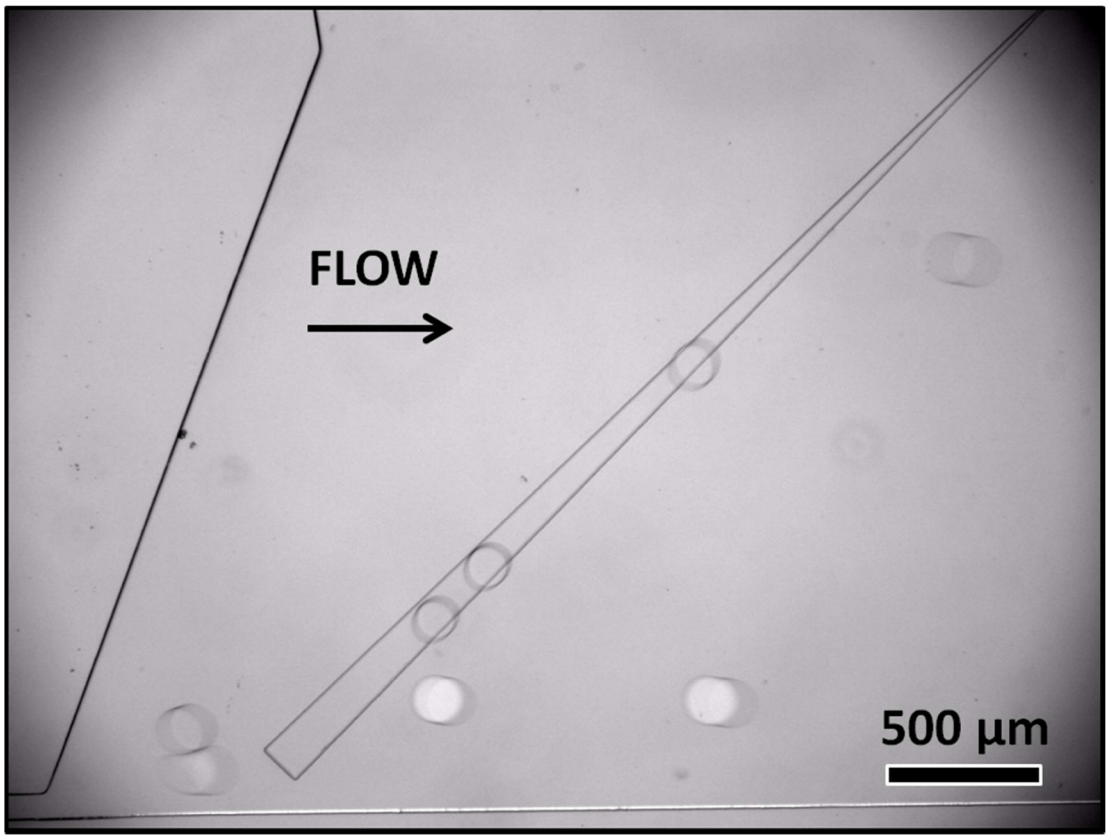

Figure 4.

Selection of isozymes based on enzymatic activity for the hydrolysis of phenyl acetate (0.244M). White droplets contain Esterase Isoenzyme 4 while clear droplets contain Esterase Isoenzyme 5 (both at 3.75 µM). Esterase Isoenzyme 5 has greater activity producing more acidic product, leading to a lower droplet pH and higher interfacial tension. Esterase 5 droplets follow the rail and have a different lateral position in the channel as compared to droplets containing Isoenzyme 4 with lower enzyme activity.